crystalline phase or the conversion of amorphous calcium phosphate to hydroxyapatite. However, the aggregate does provide a locally high concentration of bound mineral ions, so that degradation of the protein would lead to spontaneous precipitation of a mineral phase or to growth of preexisting mineral. Alternatively, if phosphophoryn is secreted as a monomer and immobilized on the collagen fibrils in the dentin matrix before aggregation can occur, then conceivably the protein could catalyze the formation of hydroxyapatite crystals. In vitro studies alone do not give enough information to define the role of high-capacity calcium-binding proteins in the mineralization process. Intracellular pathways for phosphophoryn mineralization and aggregation must also be examined.

ACKNOWLEDGMENTS

I am grateful to Sam Marsh for writing the program to calculate mineral ion activities.

REFERENCES

Bates, R. G. (1951) *J. Res. Natl. Bur. Stand. (U.S.) 47*, 127-134.
Bates, R. G., & Acree, S. F. (1943) *J. Res. Natl. Bur. Stand. (U.S.) 30*, 129-155.
Betts, F., Blumenthal, N. C., & Posner, A. S. (1981) *J. Cryst. Growth 53*, 63-73.
Chughtai, A., Marshall, R., & Nancollas, G. H. (1968) *J. Phys. Chem. 72*, 208-211.
Crenshaw, M. A. (1982) in *Biological Mineralization and Demineralization* (Nancollas, G. H., Ed.) pp 243-258, Springer-Verlag, New York.
Davies, C. W. (1962) *Ion Association*, Butterworth, London.
Dimuzio, M. T., & Veis, A. (1978) *J. Biol. Chem. 253*, 6845-6852.
Glimcher, M. J. (1981) in *The Chemistry and Biology of Mineralized Tissues* (Veis, A., Ed.) pp 618-673, Elsevier, New York.
Holt, C. (1982) *J. Dairy Res. 49*, 29-38.
Koutsoukos, P., Amjad, Z., Tomson, M. B., & Nancollas, G. H. (1980) *J. Am. Chem. Soc. 102*, 1553-1557.
Lee, S. L., Veis, A., & Glonek, T. (1977) *Biochemistry 16*, 2971-2979.
Lee, S. L., Glonek, T., & Glimcher, M. J. (1983) *Calcif. Tissue Int. 35*, 815-818.
Linde, A., Bhown, M., & Butler, W. T. (1980) *J. Biol. Chem. 255*, 5931-5942.
Lussi, A., Crenshaw, M. A., & Linde, A. (1988) *J. Dent. Res. 67*, 180.
Maier, G. D., Lechner, J. H., & Veis, A. (1983) *J. Biol. Chem. 258*, 1450-1455.
Marsh, M. E. (1988) in *Origin, Evolution and Modern Aspects of Biomineralization in Plants and Animals* (Crick, R. E., Ed.) Plenum, New York (in press).
Marsh, M. E., & Sass, R. L. (1984) *Biochemistry 23*, 1448-1456.
Meyer, J. L., & Eanes, E. D. (1978) *Calcif. Tissue Res. 25*, 59-68.
Nancollas, G. H. (1982) in *Biological Mineralization and Demineralization* (Nancollas, G. H., Ed.) pp 79-99, Springer-Verlag, New York.
Nawrot, C. F., Campbell, D. J., Schroeder, J. K., & Van Valkenburg, M. (1976) *Biochemistry 15*, 3445-3449.
Termine, J. D., & Conn, K. M. (1976) *Calcif. Tissue Res. 22*, 149-157.
Termine, J. D., Eanes, E. D., & Conn, K. M. (1980) *Calcif. Tissue Int. 31*, 247-251.
Veis, A. (1978) *Colston Pap. 29*, 259-272.

Analysis of Peptides for Helical Prediction†

Gene Merutka and Earle Stellwagen*
Department of Biochemistry, University of Iowa, Iowa City, Iowa 52242
Received March 22, 1988; Revised Manuscript Received July 12, 1988

ABSTRACT: Two terminally blocked peptides, acetylAETAAAKFLRQHMamide and acetyl-AETSSSRYLRQHMamide, were obtained by solid-phase synthesis, purified by reversed-phase chromatography, and characterized by fast atom bombardment mass spectrometry. Both peptides were soluble in aqueous solutions and remained monomeric over the concentration range examined. Changes in the temperature, pH, and trifluoroethanol concentration of solutions of each peptide produced changes in the far-ultraviolet circular dichroic spectrum characteristic of a two-state helix/coil transition. The limiting mean residue ellipticity of the coil and helix form of each peptide was estimated by addition of the denaturant guanidinium chloride at elevated temperature and by addition of trifluoroethanol at subzero temperatures, respectively. The midpoint for the thermal transition of the peptide SSSRY is lowered by about 30 °C relative to that of peptide AAAKF, in qualitative agreement from predictions based on helix probabilities of amino acid residues. The magnitude of the change observed in the midpoint of the thermal transitions suggests that the effect of single amino acid replacements on helix formation should be experimentally measurable.

An essential feature of the prediction of the biofunctional structure of a protein from its sequence is the accurate location of the secondary structural elements, the helices, strands, and reverse turns. Unfortunately, the confidence level in the prediction of secondary structural elements using current schemes is not very high, the best efforts being about 70% accurate. One major source of this poor performance may be the statistical values for the occurrence of each amino acid in a given secondary structure based on detailed analyses of

†This investigation was supported by U.S. Public Health Service Program Project Grant HL14388 from the National Heart, Lung and Blood Institute and by National Science Foundation Biological Instrumentation Program Grant DMB 8413658.

0006-2960/89/0428-0352$01.50/0 © 1989 American Chemical Society

Table I: Peptide Sequences

designation	sequence
S-peptide (1-19)	KETAAAKFERQHMDSSTSA
C-Peptide (1-13)	KETAAAKFERQHM
VI[a]	succinylAETAAAKFLRQHMDSamide
III[b]	acetylAETAAAKFLRAHAamide
AAAKF	acetylAETAAAKFLRQHMamide
SSSRY	acetylAETSSSRYLRQHMamide

[a] Mitchinson & Baldwin (1986). [b] Shoemaker et al. (1987).

Table II: Helix Probabilities

helix length	probability values	mean residue helix probability		
		AAAKF	SSSRY	difference
1–13	nonpositional[a]	1.23	1.07	0.16
	positional[b]	1.46	1.22	0.24
3–13	nonpositional	1.20	1.02	0.18
	positional	1.34	1.19	0.15

[a] Levitt (1978). [b] Argos & Palau (1982).

crystallographic models. These statistical values represent not only the inherent probability of each amino acid to reside in a secondary structure but also the ability of that secondary structure to tightly pack with the remainder of the protein tertiary structure. We suggest that the statistical value for the inherent preference of an amino acid in a given secondary structure may be perturbed by such packing considerations.

One way to investigate the inherent preference of an amino acid for a given secondary structure free of packing considerations would be to utilize a small peptide which could form a free-standing secondary structural element in solution. The recent reports (Shoemaker et al., 1985, 1987) of the enhancement of the helical content of analogues of the C-peptide of ribonuclease based on dipolar considerations suggest an experimental system for such a study. In this report, we have constructed the peptide acetylAETAAAKFLRQHMamide, termed peptide AAAKF (Table I), expected to be about 45% helical at 3 °C and pH 5 (Shoemaker et al., 1985), to serve as a reference peptide. As a feasibility study of the magnitude of the helix/coil perturbation, we have constructed a test peptide having five amino acid replacements selected to maximally decrease the helical content on the basis of helix probabilities while minimally perturbing dipolar and steric considerations, acetylAETSSSRYLRQHMamide, termed peptide SSSRY (Table I). As can be seen in Table II, the mean residue probability of helix formation of peptide AAAKF is predicted to be consistently higher than SSSRY, irrespective of whether position-independent (Levitt, 1978) or position-dependent (Argos & Palau, 1982) helix probability values are used. This difference is also present no matter if the helix is taken to be residues 3–13, as in the crystal structure (Wlodawar et al., 1982), or the entire sequence, 1–13, of these terminally blocked analogues. We find that the thermal dependence of the far-ultraviolet circular dichroic spectrum is markedly diminished by these simultaneous replacements, suggesting that the effect of single replacements could be experimentally evaluated with confidence.

Experimental Procedures

Materials. The peptides AAAKF and SSSRY were synthesized by Biosearch, San Rafael, CA, using a 4-methylbenzhydrylamine resin. The immobilized peptides were cleaved and deblocked with HF using anisole as a scavenger, extracted with acetic acid, and lyophilized. Each peptide preparation had an amino acid composition within 5% of that expected. Neat 2,2,2-trifluoroethanol was purchased from Aldrich Chemical Co. Purified guanidinium chloride was purchased from Heico Chemicals. Fluorinert FC-84 was obtained from 3M.

Methods. Each peptide preparation was purified by reversed-phase chromatography using a 7 × 300 mm Hamilton PRP-1 column and an IBM LC/9533 chromatograph. About 18 mg of peptide AAAKF in 300 μL of water was injected into a gradient consisting of 20–50% acetonitrile in 0.1% trifluoroacetic acid generated in 30 min at a flow rate of 1 mL/min at ambient temperature. The column effluent was monitored at 220 nm using an ISCO Model V4 absorbance detector and collected in 0.5-mL fractions. Fractions containing the major effluent component were lyophilized individually and dissolved in water. An aliquot from each fraction was injected into a 4.6 × 100 mm C18 Phenomenex IB-SIL column containing 3-μm particles. The injected peptide was subjected to a gradient between 20 and 35% acetonitrile in 0.1% trifluoroacetic acid generated in 10 min at a flow rate of 1 mL/min. All the fractions examined in the Hamilton column effluent found to be at least 90% homogeneous upon rechromatography using the Phenomenex column were pooled and lyophilized. All gradients contained 10% less acetonitrile when peptide SSSRY was purified.

Fast atom bombardment mass spectrometry was performed using a VG analytical ZAB-HF mass spectrometer and an Ion Tech 11-NF saddlefield atom gun, both located in he University of Iowa Mass Spectrometry Facility. Measurements were obtained by using xenon gas, an equivalency of 8 kV with 1.5-mA current, and a magic bullet matrix consisting of a 4:1 mixture of dithioerythritol and dithiothreitol. The spectra were calibrated using Cs_6I_5 and Cs_7I_6.

Circular dichroic measurements were obtained by using an Aviv Associates Model 60DS spectropolarimeter located in the University of Iowa Protein Structure Facility. Optical cells having a path length between 1 and 10 mm were placed in a thermostable cell holder and brought to the desired temperature by circulation of either ethylene glycol/water or 1-propanol from a Neslab Model RTE-4DD refrigerated bath or by circulation of FC-84 Fluorinert from a FTS Systems Model RC-200-80 recirculating cooler. The sample temperature was measured by using an Omega Engineering digital thermometer with a type K thermocouple and was accurate to within 1 °C throughout the experimental range. The concentration of amino acids in the sample was determined in triplicate by using the ninhydrin assay described by Troll and Cannan (1953) following base hydrolysis performed as described by Fruchter and Crestfield (1965). These procedures were standardized by using leucine in the concentration range 0–1 μmol.

Results

Each supplied peptide preparation contained a major component when examined by reversed-phase chromatography as shown by the upper profiles of Figure 1. Fractionation of the effluent from each column increased the relative population of the major component as illustrated in the lower profiles of Figure 1. The mass spectrum for fractionated peptide AAAKF, shown in Figure 2, displays a major component having a mass of 1515 which corresponds with the mass calculated for peptide AAAKF complexed with a single hydrogen. The spectrum for the fractionated peptide SSSRY, also shown in Figure 2, displays two major components having

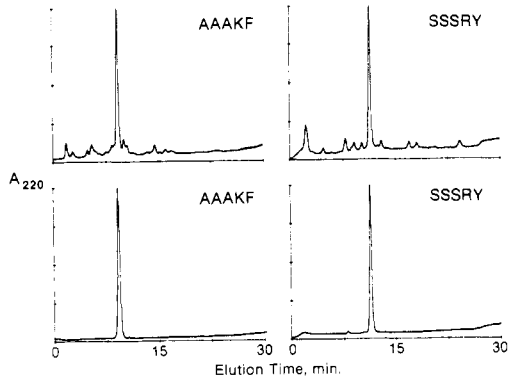

FIGURE 1: Chromatographic elution profiles. The left panels illustrate elution profiles observed for peptide AAAKF, and the right panels illustrate the elution profiles observed for peptide SSSRY from a PRP-1 Hamilton column using an acetonitrile gradient. The upper profiles were observed following injection of each supplied peptide preparation, and the lower profiles were observed following injection of the fractionated preparation. The time at the left edge of each panel represents the arrival of the beginning of the acetonitrile gradient at the absorbance detector, and the right edge of each panel represents the completion of the gradient at that location. The ordinate represents the absorbance measured at 220 nm and is scaled so that the major component in each elution profile has the same amplitude.

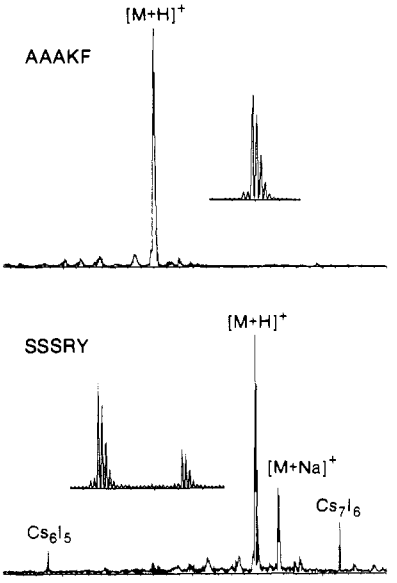

FIGURE 2: Mass spectral analyses. The mass spectrum for the peptide AAAKF is illustrated in the upper portion of the main figure, and the mass spectrum for peptide SSSRY is illustrated in the lower portion of the main figure. The ionic components corresponding to each peptide combined with either hydrogen or sodium are identified. The calibration compounds Cs_6I_5 and Cs_7I_6 having mass values of 1432 and 1692, respectively, are also identified. The inserts illustrate the mass spectrum of the major component(s) in each peptide preparation on a 3.7-fold expanded mass/charge scale to display the isotope distribution.

mass values of 1607 and 1629 which correspond with those calculated for peptide SSSRY complexed with a single proton or a single sodium cation, respectively. No significant population of components having mass/charge values between 1100 and 1400 was evident in the spectra of either peptide.

The far-ultraviolet circular dichroic spectra of peptide AAAKF and peptide SSSRY exhibit minima at 207 ± 1 and 220 ± 1 nm in NaCl solutions buffered at pH 5 and maintained at low temperature, as shown in Figure 3. Minima at these wavelengths are characteristic for peptide solutions having a significant population of α helix. The dichroic spectrum of each peptide was independent of concentration over the range 5–235 μM. Single-wavelength measurements

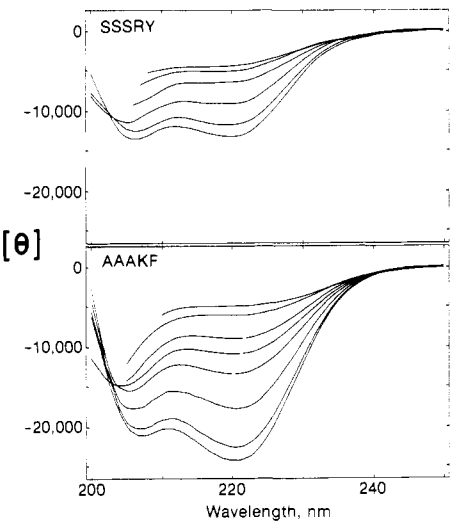

FIGURE 3: Effect of temperature on the far-ultraviolet dichroic spectra of the peptides in 5 M NaCl. The upper panel illustrates spectra for peptide SSSRY obtained in −30, −23, −7, 15, 40, and 55 °C reading upward at 220 nm. The lower panel illustrates spectra for peptide AAAKY obtained at −30, −24, −12, 0, 9, 17, 41, and 78 °C reading upward at 220 nm. All solutions contained between 67 and 120 μM peptide, 5 M NaCl, and 10 mM acetate buffer, pH 5, and were measured in a cell having an optical path of 2 mm. The mean residue ellipticity, $[\theta]$, has the units deg cm^2 dmol^{-1}.

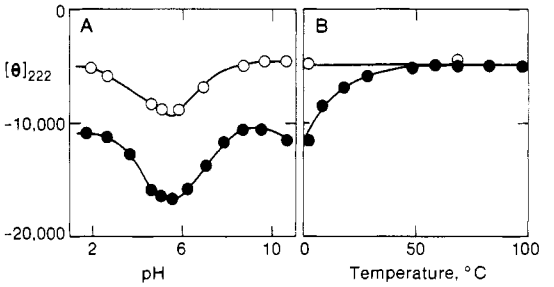

FIGURE 4: Effect of pH and temperature on the mean residue ellipticity at 222 nm in 0.1 M NaCl. Panel A illustrates the pH dependence of the ellipticity values observed at 2 °C, and panel B illustrates the temperature dependence of the ellipticity values observed at pH 10.6. Open symbols indicate ellipticity values observed for peptide SSSRY and closed circles for peptide AAAKF. All measurements were obtained by using a cell with an optical path of 10 mm and a solution containing 45 μM peptide in 0.1 M NaCl and 1 mM each of citrate, phosphate, and borate buffers. The mean residue ellipticity, $[\theta]$, has the units deg cm^2 dmol^{-1}.

are reported at 222 nm rather than at the helical minimum 220 nm to facilitate comparison with previously reported values.

Addition of acid or base to each peptide solution changes the dichroic spectrum by diminishing the ellipticity values observed at 207 and 220 nm while maintaining isodichroic ellipticity values at 204 nm and above 245 nm. Such changes are characteristic of a two-state transition. The pH dependence of the mean residue ellipticity of each peptide observed at 222 nm is bell-shaped, having inflection points at pH 4 and 7 and a maximal negative value between pH 5 and 6, as shown in Figure 4A. This bell-shaped dependence is characteristic of analogues of the C-peptide (Shoemaker et al., 1985) and likely reflects the interaction of the carboxylate of glutamate-3 and the protonated imidazole of histidine-12 with the helix dipole. Raising the temperature of the solution of peptide AAAKF buffered at pH 10.6 decreases the mean residue ellipticity of this peptide to a limiting value observed above 50 °C, as shown in Figure 4B. By contrast, the mean residue ellipticity of peptide SSSRY at pH 10.6 does not change with temperature and has the same limiting value as that observed for peptide

Table III: Comparative Dichroic Values[a]

variable				peptide			
parameter	solvent	temp (°C)	pH	VI	III	AAAKF	SSSRY
$[\theta]_{222}$	0.1 M NaCl	2	2	−10.0	−10.4	−10.9	−5.2
	0.1 M NaCl	2	5	−13.1	−13.2	−14.8	−8.8
	0.1 M NaCl	2	10	−10.0	−7.6	−10.5	−4.6
	5.0 M NaCl	2	5			−12.7	−7.7
	≥20% TFE	2	5			−22.7	−17.5
$[\theta]_{222}$	H_2O	>65	5			−6.1	−5.1
	0.1 M NaCl	>65	5	−4.6	−4.8	−6.1	−4.8
	5.0 M NaCl	>65	5			−4.7	−4.4
TIDP	0.1 M NaCl		5		202	203	203
	5.0 M NaCl		5			203	203
	83% TFE		5			201	201
$[\theta]_{TIDP}$	0.1 M NaCl		5		−13.3	−11.3	−13.3
	5.0 M NaCl		5			−14.4	−10.9
	83% TFE		5			−9.0	−5.9

[a] All solvents except those at pH 2 and 10 contained 10 mM acetate buffer, pH 5.0. The mean residue ellipticity, $[\theta]$, has the units degees centimeter squared per decimole × 10^{-3}. The thermal isodichroic point, TIDP, has the units nanometers. The concentration of 2,2,2-trifluoroethanol, TFE, is expressed in mole percent. The values for peptide VI were obtained from Mitchinson and Baldwin (1986) and those for peptide III from Shoemaker et al. (1987).

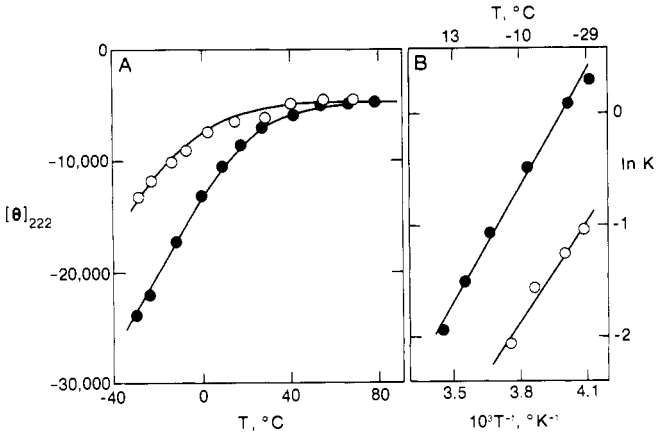

FIGURE 5: Effect of temperature on the mean residue ellipticity measured at 222 nm. The open symbols indicate measurements obtained by using the peptide SSSRY, and the closed symbols indicate measurements obtained by using the peptide AAAKF. All solutions contained between 21 and 120 μM peptide, 5 M NaCl, and 10 mM acetate buffer, pH 5.0. The mean residue ellipticity, $[\theta]$, has the units deg cm^2 dmol^{-1}. The van't Hoff plot (panel B) was constructed assuming a two-state transition have a limiting value for the coil form of −4400 and 4700 for peptides SSSRY and AAAKF, respectively, and a limiting value for the helical form of −38 500 for both peptides.

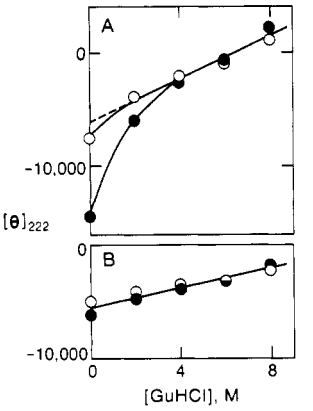

FIGURE 6: Effect of guanidinium chloride on the mean residue ellipticity at 222 nm. Panel A illustrates measurements made at 20 °C and panel B at 70 °C. All solutions contained between 182 and 190 μM peptide, 10 mM acetate, and the indicated concentrations of guanidinium chloride, GuHCl, adjusted to pH 5. The open symbols indicate measurements obtained with peptide SSSRY, and the closed symbols indicate measurements obtained with peptide AAAKF. The straight line in panel A represents a linear regression of all experimental values obtained in greater than 3 M denaturant. The straight line in panel B represents a linear regression of all experimental values. All measurements were made in a cell having an optical path of 1 mm. The mean residue ellipticity, $[\theta]$, has the units deg cm^2 dmol^{-1}.

AAAKF at pH 10.6 and elevated temperature.

Increasing the temperature of solutions of each peptide maintained at pH 5 also changes the far-ultraviolet dichroic spectra in a manner characteristic for a two-state transition as illustrated in Figure 3. Unfortunately, the dichroic spectrum cannot be observed below 210 nm in concentrated NaCl at elevated temperatures because of the thermal dependence of the absorbance of this solvent. Absorbance is not a problem at lower NaCl concentrations where an isodichroic point is evident at 203 nm at all temperatures. The dichroic features observed for peptide AAAKF compare favorably with those previously reported (Mitchinson & Baldwin, 1986; Shoemaker et al., 1987) for peptides III and VI as shown in Table III. The shape of the limiting dichroic spectra at temperatures in excess of 65 °C suggests that the thermal changes represent a helix/coil transition where the coil form is considered to have an unordered conformation. The thermal dependence of the mean residue ellipticity for peptides AAAKF and SSSRY was observed in 5 M NaCl to facilitate measurements at subzero centrigrade temperatures. As seen in Figure 5A, the thermal transition for peptide SSSRY appears to occur in a lower temperature range than that observed for peptide AAAKF.

An effort was made to establish the limiting mean residue ellipticity values of the helix/coil transition observed at 222 nm in order to determine the midpoint or melting temperature for each peptide. The limiting value for the coil form was examined by using the protein denaturant guanidinium chloride, and the results are shown in Figure 6. If it is assumed that the mean residue ellipticity exhibits a monotonic dependence on denaturant concentration outside a conformational transition zone, a limiting ellipticity of −5800 ± 400 deg cm^2 dmol^{-1} can be predicted for the unordered form of both peptides at 20 and at 70 °C.

Addition of NaCl to lower the freezing point of the peptide solutions did not reveal the limiting mean residue ellipticity value for the helical form of either peptide as shown in Figure 5A. Replacement of NaCl with $NaClO_4$, which has quite different lyotropic properties, shifted the thermal transition of each peptide to higher temperatures by about 10 °C but also failed to define the limiting ellipticity value for the helical form of each peptide. The helix stabilizing reagent 2,2,2-trifluoroethanol was then used to search for the limiting ellipticity values. Addition of increasing concentrations of

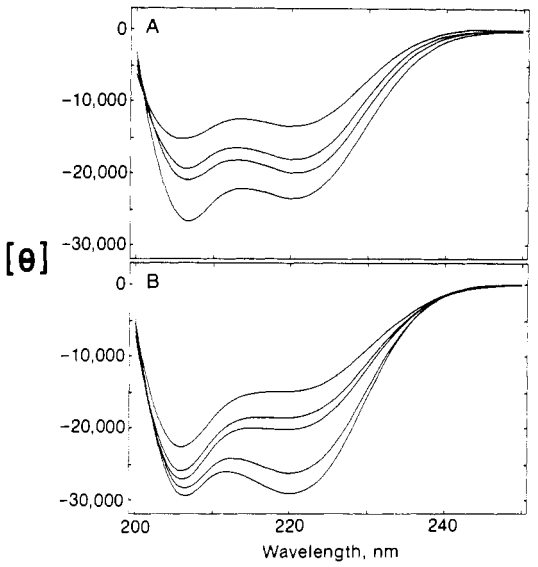

FIGURE 7: Effect of trifluoroethanol on the far-ultraviolet dichroic spectrum of peptide AAAKF. Panel A illustrates spectra observed using solution maintained at 2 °C and containing 10, 5, 3, and 0 mol % trifluoroethanol, reading upward at 220 nm. Panel B illustrates the effect of temperature on the spectrum observed using a solution containing 83 mol % trifluoroethanol. The temperatures were −55, −30, 19, 30, and 55 °C, reading upward at 220 nm. All spectra were obtained using solutions containing 148 μM peptide in 10 mM acetate buffer, pH 5.0, placed in a cell having an optical path of 10 mm. The mean residue ellipticity at 222 nm, [θ], has the unit deg cm^2 dmol^{-1}.

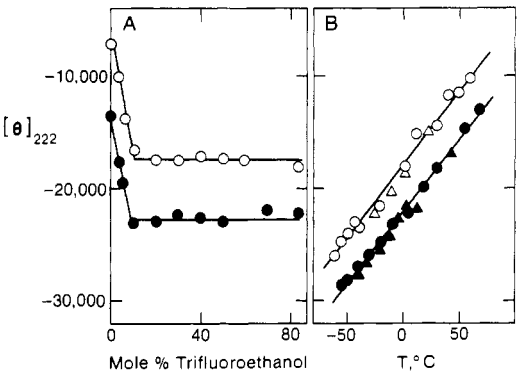

FIGURE 8: Effect of trifluoroethanol on the mean residue ellipticity at 222 nm. The open symbols indicate measurements obtained with peptide SSSRY, and the closed symbols indicate measurements obtained with peptide AAAKF. Panel A illustrates the dependence of ellipticity on trifluoroethanol concentration observed at 2 °C. Panel B illustrates the effect of temperature on the ellipticity observed in 69 mol % trifluoroethanol (triangles) or in 83 mol % trifluoroethanol (circles). All solutions contained between 148 and 184 μM peptide and 10 mM acetate buffer, pH 5.0. Measurements were obtained using a cell having an optical path of 10 mm. The mean residue ellipticity, [θ], has the units deg cm^2 dmol^{-1}.

trifluoroethanol changes the dichroic spectrum of each peptide in a manner characteristic for a helix/coil transition as illustrated for peptide AAAKF in Figure 7A. The mean residue ellipticity of each peptide at 222 nm decreases linearly with increasing trifluoroethanol concentration until a minimal value is attained in 10 mol % reagent as shown in Figure 8A. This concentration of trifluoroethanol has been found to complete a major conformational transition in S-peptide as well (Nelson & Kallenbach, 1986). The dependence of the minimal value observed in excess of 10 mol % trifluoroethanol on temperature was investigated by using peptide solutions containing 83 mol % trifluoroethanol. This concentration was selected to facilitate measurement at the lowest temperature at which trifluoroethanol/water mixtures remain liquid (Halocarbon, 1979). The changes in dichroic spectra of the peptides observed in 83 mol % trifluoroethanol with temperature are characteristic for a helix/coil transition, as illustrated for peptide AAAKF in Figure 7B. Unfortunately, trifluoroethanol appears to decrease the cooperativity of the peptide helix/coil transitions such that only the central portion of the transition can be observed in the thermal range in which the solutions remain liquid as illustrated in Figure 8B. Nevertheless, it can be concluded that the thermal transitions of the two peptides have the same cooperativity in excess trifluoroethanol and that their transition midpoints are separated by about 33 °C.

Discussion

The amino acid composition, reversed-phase chromatography, and mass spectral results taken together indicate that each sample contains a single peptide, that only the desired amino acids are present, that the N-terminus is acetylated and the C-terminus amidated, and that the protecting groups used in peptide synthesis have been removed. Use of mass spectral analysis is particularly noteworthy since acetylation of the N-terminus of each peptide precludes determination of the peptide sequence by conventional chemical procedures. The far-ultraviolet dichroic properties of peptide AAAKF in 0.1 M NaCl are very comparable with those of synthetic peptides of similar sequence previously characterized, as shown in Table III. Such comparisons suggest that procedures used in the measurements reported in this paper are reliable as well.

The dichroic spectra of both peptides observed at temperatures in excess of 65 °C are negative and relatively featureless in the range 210–240 nm as illustrated in Figure 3. Similar spectra are observed for proteins in guanidinium chloride or urea concentrations in excess of their conformational transitions (Morrisett & Broomfield, 1971; Cortijo et al., 1973; Litman et al., 1973; Hon-nami & Oshima, 1979; Rossi et al., 1983; Rudolph et al., 1986). By contrast, the dichroic spectra observed at low temperatures in the presence of salt or trifluoroethanol exhibit the features characteristic for the presence of an α helix as illustrated in Figures 3 and 7. The persistence of a common isodichroic wavelength in response to changes in temperature, pH, or trifluoroethanol concentration, as illustrated in Figures 3 and 7 and in Table III, indicates that a two-state helix/coil transition is observed. However, these dichroic measurements cannot distinguish whether the structural unit in the two-state transition is an individual residue or all the residues in a peptide acting in concert. Recent NMR measurements (Kuwajima & Baldwin, 1983; Rico et al., 1986) suggest that all the residues in the S-peptide of ribonuclease can act in concert in a helix/coil transition. Accordingly, it will be assumed in this discussion that the dichroic measurements described here represent a concerted helix/coil transition of all the residues in a peptide.

The mean residue ellipticity of the coil form of each peptide at 222 nm, −5200 ± 700 deg cm^2 dmol^{-1} (Table III and Figure 6), is within the range of values observed for denatured proteins, −3300 ± 1200 deg cm^2 dmol^{-1}, obtained by using comparable conditions (Nojima et al., 1977, 1978; Ahmad & Bigelow, 1979; Vita & Fontana, 1982; Dalzoppo et al., 1985; Ikeguchi et al., 1986). The mean residue ellipticity of the helical form of each peptide at 222 nm could not be established experimentally owing to the thermal range of the liquid form of the solvents employed. However, the dichroic measurements in 83 mol % trifluoroethanol (Figure 8B) indicate that the helical form of each peptide must have an ellipticity more negative than −29 200 deg cm^2 dmol^{-1}, the value for the 3–13 helix in S-peptide estimated from circular dichroic measure-

ments of the complexation of S-peptide with S-protein (Shoemaker et al., 1985). Accordingly, for this discussion, it will be assumed that the helical form of both peptides has an ellipticity at 222 nm of −38 500 deg cm^2 $dmol^{-1}$, the mean of the values obtained by direct measurement of helical homopolymers (Holzwarth & Doty, 1965; Greenfield & Fasman, 1969; Fillipi et al., 1978; Toniolo et al., 1979) and by deconvolution of measurements of native proteins (Chang et al., 1978). The more negative value assumed for the helical form of the peptides used in this study in comparison with the S-peptide of ribonuclease may reflect the blockage of the N-terminus which may accommodate all 13 residues in the helical form.

A van't Hoff plot of the thermal transition observed for each peptide in 5 M NaCl is illustrated in Figure 5B. This plot suggests that the helix/coil transition for each peptide has the same cooperativity and that the midpoints of the individual transitions differ by about 30 °C. This statement is more convincingly documented by the measurements in 83 mol % trifluoroethanol (Figure 8B) where the central portion of the transition observed for each peptide is described with more certainty. The slopes of both lines in Figure 8B are clearly parallel, indicating the transitions of both peptides in trifluoroethanol have the same cooperativity. The limiting ellipticity observed for each peptide in excess trifluoroethanol at low temperature suggests that at least residues 3–13 in each peptide are helical (Shoemaker et al., 1987) and that all the residues are likely helical.

These comparisons suggest that changes in a peptide helix/coil transition resulting from single amino acid replacements can be observed with precision since the replacements examined here caused an average change in thermal transition of about 6 °C per residue. Accordingly, it should be possible to use small monomeric peptides to experimentally refine both the inherent helix probabilities of each amino acid residue and the algorithms used to predict helix nucleation and growth. Clearly, such a study must involve a multitude of replacements to investigate the effect of neighboring residues in the sequence and in the helix on these parameters. It is anticipated that the use of concentrated salt and trifluoroethanol concentrations at low temperatures will be useful to these measurements. It should be noted that each of the solvent variables—pH, salt concentration, trifluoroethanol concentration, and temperature—only appears to shift the helix/coil equilibrium by an incremental amount and that these variables must be managed in concert to drive the equilibrium to essentially populate only one conformational form of a peptide.

Registry No. AAAKF, 117940-96-2; SSSRY, 117940-97-3.

References

Ahmad, F., & Bigelow, C. C. (1979) *J. Mol. Biol. 131*, 607–617.

Argos, P., & Palau, J. (1982) *Int. J. Pept. Protein Res. 19*, 380–393.

Chen, Y.-H., Yang, J. T., & Chau, K. H. (1974) *Biochemistry 13*, 3350–3359.

Cortijo, M., Panijpan, B., & Gratzer, W. B. (1973) *Int. J. Pept. Protein Res. 5*, 179–186.

Dalzoppo, D., Vita, C., & Fontana, A. (1985) *J. Mol. Biol. 182*, 331–340.

Fruchter, R. G., & Crestfield, A. M. (1965) *J. Biol. Chem. 240*, 3868–3874.

Greenfield, N., & Fasman, G. D. (1969) *Biochemistry 8*, 4108–4116.

Halocarbon Products Corp. (1979) *Trifluoroethanol*, Hackensack, NJ.

Hon-nami, K., & Oshima, T. (1979) *Biochemistry 18*, 5693–5697.

Ikeguchi, M., Kuwajima, K., Mitani, M., & Sugai, S. (1986) *Biochemistry 25*, 6965–6972.

Levitt, M. (1978) *Biochemistry 17*, 4277–4285.

Litman, G. W., Litman, R. S., Good, R. A., & Rosenberg, A. (1973) *Biochemistry 12*, 2004–2011.

Mitchinson, C., & Baldwin, R. L. (1986) *Proteins: Struct. Funct. Genet. 1*, 23–33.

Morrisett, J. D., & Broomfield, C. A. (1971) *J. Am. Chem. Soc. 93*, 7297–7304.

Nelson, J. W., & Kallenbach, N. R. (1986) *Proteins: Struct. Funct. Genet. 1*, 211–217.

Nojima, H., Ikai, A., Oshima, T., & Noda, H. (1977) *J. Mol. Biol. 116*, 429–442.

Nojima, H., Hon-nami, K., Oshima, T., & Noda, H. (1978) *J. Mol. Biol. 122*, 33–42.

Rossi, V., Grandi, C., Dalzoppo, D., & Fontana, A. (1983) *Int. J. Pept. Protein Res. 22*, 239–250.

Rudolph, R., Fuchs, I., & Jaenicke, R. (1986) *Biochemistry 25*, 1662–1669.

Saxena, V. P., & Wetlaufer, D. B. (1971) *Proc. Natl. Acad. Sci. U.S.A. 68*, 969–972.

Shoemaker, K. R., Kim, P. S., & Baldwin, R. L. (1985) *Proc. Natl. Acad. Sci. U.S.A. 82*, 2349–2353.

Shoemaker, K. R., Kim, P. S., York, E. J., Stewart, J. M., & Baldwin, R. L. (1987) *Nature (London) 326*, 563–567.

Troll, W., & Cannan, R. K. (1953) *J. Biol. Chem. 200*, 803–811.

Vita, C., & Fontana, A. (1982) *Biochemistry 21*, 5196–5202.

Wlodawer, A., Bott, R., & Sjölin, L. (1982) *J. Biol. Chem. 257*, 1325–1332.